arXiv:1209.2044v1 [physics.gen-ph] 5 Sep 2012

QCD modified ghost scalar field dark energy models

K. Karami*, M. Mousivand
Department of Physics, University of Kurdistan, Pasdaran St., Sanandaj, Iran

September 11, 2012

Abstract

Within the framework of FRW cosmology, we study the QCD modified ghost scalar field models of dark energy in the presence of both interaction and viscosity. For a spatially non-flat FRW universe containing modified ghost dark energy (MGDE) and dark matter, we obtain the equation of state of MGDE, the deceleration parameter as well as a differential equation governing the MGDE density parameter. Furthermore, we reconstruct both the dynamics and potentials of the quintessence, tachyon, K-essence and dilaton scalar field DE models according to the evolution of the MGDE density.

PACS numbers: 98.80.−k, 95.36.+x
Keywords: Dark energy theory, Scalar filed models

---

*KKarami@uok.ac.ir

1 Veneziano MGDE paradigm

The Veneziano MGDE density is given by [1]

$$\rho_D = \alpha H + \beta H^2, \tag{1}$$

where α and β are two constants, roughly of order of $\Lambda^3_{\rm QCD}$ and $\Lambda^2_{\rm QCD}$, where $\Lambda_{\rm QCD} \sim 100$ MeV is the QCD mass scale and H is the Hubble parameter. The original version of the Veneziano GDE, i.e. $\rho_D = \alpha H$, has been already studied in the literature [2, 3, 4, 5, 6, 7, 8, 9, 10]. Note that in Eq. (1), the term proportional to H^2 becomes important during the early evolution of the universe and behaves like the early DE [1].

In a spatially non-flat FRW universe filled with MGDE density ρ_D and DM energy density $\rho_{\rm m}$, the first Friedmann equation within the framework of Einstein gravity reads

$$H^2 + \frac{k}{a^2} = \frac{1}{3M_P^2}\,(\rho_D + \rho_{\rm m}), \tag{2}$$

where the scalar curvature $k = 0, 1, -1$ denote a flat, closed and open FRW universe, respectively. Also $M_P = (8\pi G)^{-1/2}$ is the reduced Planck mass.

Using the fractional energy densities

$$\Omega_{\rm m} = \frac{\rho_{\rm m}}{\rho_{\rm cr}} = \frac{\rho_{\rm m}}{3M_P^2 H^2}, \quad \Omega_D = \frac{\rho_D}{\rho_{\rm cr}} = \frac{\rho_D}{3M_P^2 H^2}, \quad \Omega_k = \frac{k}{a^2 H^2}, \tag{3}$$

the Friedmann equation (2) can be rewritten as

$$1 + \Omega_k = \Omega_D + \Omega_{\rm m}. \tag{4}$$

Substituting Eq. (1) into the middle relation of Eq. (3) gives

$$\Omega_D = \frac{\alpha}{3M_P^2 H} + 1 - \gamma, \tag{5}$$

where

$$\gamma = 1 - \frac{\beta}{3M_P^2}. \tag{6}$$

Inserting this into the last relation of Eq. (3) yields

$$\Omega_k = \frac{\Omega_{k_0}}{(\Omega_{D_0} + \gamma - 1)^2}\left(\frac{\Omega_D + \gamma - 1}{a}\right)^2, \tag{7}$$

where we take $a_0 = 1$ for the present time and the subscript "0" denotes the present value of a quantity.

Following the observational evidences we extend our study to the case in which the MGDE has a bulk viscosity property [11] and also interact with DM [12]. In the presence of bulk viscosity and interaction, the energy densities of MGDE and DM do not conserve separately and continuity equations take the forms

$$\dot{\rho}_D + 3H(1 + \omega_D)\rho_D = 9H^2\xi - Q, \tag{8}$$

$$\dot{\rho}_{\rm m} + 3H\rho_{\rm m} = Q, \tag{9}$$

where $\omega_D = p_D/\rho_D$ is the equation of state (EoS) parameter of MGDE. Also $\xi = \epsilon H^{-1}\rho_D$ is the bulk viscosity coefficient with the viscosity constant ϵ and $Q = 3b^2H(\rho_D + \rho_{\rm m})$ is the interaction term with the coupling constant b^2.

Taking time derivative of Eq. (2) and using Eqs. (3), (4), (8) and (9) one can get

$$\frac{\dot{H}}{H^2} = -\frac{3}{2}\left[1 + \frac{\Omega_k}{3} + (\omega_D - 3\epsilon)\Omega_D\right]. \tag{10}$$

Taking time derivative of Eq. (1), using (10), and substituting the obtained result into Eq. (8) gives the EoS parameter of the interacting viscous MGDE as

$$\omega_D = \frac{1}{\Omega_D - \gamma - 1}\left[1 - \frac{\Omega_k}{3} + \frac{\gamma - 1}{\Omega_D}\left(1 + \frac{\Omega_k}{3}\right) + 2b^2\left(\frac{1 + \Omega_k}{\Omega_D}\right)\right] + 3\epsilon. \tag{11}$$

For the deceleration parameter

$$q = -1 - \frac{\dot{H}}{H^2}, \tag{12}$$

replacing Eq. (11) into (10) gives

$$q = \frac{\gamma + 2(\Omega_D - 1) - \Omega_k + 3b^2(1 + \Omega_k)}{\Omega_D - \gamma - 1}. \tag{13}$$

Taking the derivative of Eq. (36) with respect to $\ln a$ and using Eqs. (10) and (11) gives

$$\frac{{\rm d}\Omega_D}{{\rm d}\ln a} = 3\left(\frac{\Omega_D + \gamma - 1}{\Omega_D - \gamma - 1}\right)\left[\Omega_D - 1 - \frac{\Omega_k}{3} + b^2(1 + \Omega_k)\right]. \tag{14}$$

It is interesting to note that Eqs. (13) and (14) show that the deceleration and MGDE density parameters are independent of viscosity constant.

We solve the differential equation governing the MGDE density parameter, Eq. (14), numerically. In Fig. 1, variation of the MGDE density parameter Ω_D versus redshift $z = \frac{1}{a} - 1$ for different coupling constants b^2 is plotted. Figure 1 shows that: i) For a given b^2, Ω_D increases during history of the universe. ii) At early and late times, Ω_D increases and decreases, respectively, with increasing b^2.

In Fig. 2 we plot the evolutionary behavior of the deceleration parameter, Eq. (13), for different b^2. Figure 2 presents that: i) the universe transitions from a matter dominated epoch at early times to the de Sitter phase, i.e. $q = -1$, in the future, as expected. The result for $b^2 = 0$ is in agreement with that obtained by [1]. ii) For $b^2 = 0.0$, 0.02 and 0.04 at $z = 0.75$, 0.91 and 1.10, respectively, we have a cosmic deceleration $q > 0$ to acceleration $q < 0$ transition which is compatible with the observations [13]. iii) For a given z, although q decreases with increasing b^2, in the far future q becomes independent of b^2.

The variation of the EoS parameter of interacting viscous MGDE, Eq. (11), for different coupling b^2 and viscosity ϵ constants is plotted in Figs. 3, 4 and 5. Figures 3 and 4 illustrate that: i) in the absence of viscosity ($\epsilon = 0$), $\omega_D(z)$ varies from the quintessence phases ($\omega_D > -1$) to the phantom regime ($\omega_D < -1$). ii) In the absence of interaction ($b^2 = 0$), $\omega_D(z)$ varies from $\omega_D > -1$ to $\omega_D = -1$, which is similar to the freezing quintessence model [14]. iii) For a given z, ω_D decreases and increases with increasing b^2 and ϵ, respectively. Note that the result for $b^2 = \epsilon = 0$ is in accordance with that obtained by [1]. Figures 5 shows that the interaction and viscosity have opposite effects on ω_D.

In the next sections, we establish a correspondence between the MGDE and various scalar field models by identifying their respective energy densities and equations of state and then reconstruct both the dynamics and potential of the field.

2 Quintessence MGDE

The quintessence scalar field energy density and pressure are given by [15]

$$\rho_Q = \frac{1}{2}\dot{\phi}^2 + V(\phi), \tag{15}$$

$$p_Q = \frac{1}{2}\dot{\phi}^2 - V(\phi). \tag{16}$$

The quintessence EoS parameter takes the form

$$\omega_Q = \frac{p_Q}{\rho_Q} = \frac{\dot{\phi}^2 - 2V(\phi)}{\dot{\phi}^2 + 2V(\phi)}. \tag{17}$$

Identifying Eq. (17) with the EoS parameter of interacting viscous MGDE (11), $\omega_Q = \omega_D$, and also equating Eq. (15) with (1), $\rho_Q = \rho_D$, one can get

$$V(\phi) = \frac{1}{2}(1 - \omega_D)\rho_D, \tag{18}$$

$$\dot{\phi}^2 = (1 + \omega_D)\rho_D. \tag{19}$$

Inserting Eqs. (1) and (11) into the above equations, one can get the quintessence potential and kinetic energy as

$$V(\phi) = \frac{\alpha^2 \Omega_D}{6M_P^2(\Omega_D + \gamma - 1)^2}\left[\frac{\Omega_D - \gamma - 2 + \frac{\Omega_k}{3} - \left(\frac{\gamma-1}{\Omega_D}\right)\left(1 + \frac{\Omega_k}{3}\right) - 2b^2\left(\frac{1+\Omega_k}{\Omega_D}\right)}{\Omega_D - \gamma - 1} - 3\epsilon\right], \tag{20}$$

$$\dot{\phi}^2 = \frac{\alpha^2 \Omega_D}{3M_P^2(\Omega_D + \gamma - 1)^2}\left[\frac{\Omega_D - \gamma - \frac{\Omega_k}{3} + \left(\frac{\gamma-1}{\Omega_D}\right)\left(1 + \frac{\Omega_k}{3}\right) + 2b^2\left(\frac{1+\Omega_k}{\Omega_D}\right)}{\Omega_D - \gamma - 1} + 3\epsilon\right]. \tag{21}$$

Integrating this gives the modified quintessence scalar field as

$$\phi(a) - \phi(a_i) = \sqrt{3}\ M_P \int_{a_i}^{a} \sqrt{\Omega_D}\left[\frac{\Omega_D - \gamma - \frac{\Omega_k}{3} + \left(\frac{\gamma-1}{\Omega_D}\right)\left(1 + \frac{\Omega_k}{3}\right) + 2b^2\left(\frac{1+\Omega_k}{\Omega_D}\right)}{\Omega_D - \gamma - 1} + 3\epsilon\right]^{\frac{1}{2}} \frac{\mathrm{d}a}{a}. \tag{22}$$

The above integral cannot be taken analytically. But with the help of Eq. (7) and numerical solution of the differential equation (14) one can obtain the evolutionary behavior of the quintessence MGDE scalar field. In Figs. 6, 7 and 8 we plot the variation of scalar field, Eq. (22), versus redshift. Figures 6 and 7 present that: i) for a given b^2 or ϵ, ϕ increases during history of the universe. ii) For a given z, ϕ decreases and increases with increasing b^2 and ϵ, respectively. Figure 6 shows that for $b^2 = 0.0$, 0.02 and 0.04 at $z < -0.97$, -0.57 and -0.41, respectively, ϕ becomes pure imaginary, i.e. $\dot{\phi}^2 < 0$, and does not show itself in Fig. 6. For $\dot{\phi}^2 < 0$ the MGDE scalar field behaves as a phantom-type scalar field [16]. Figure 8 clarifies that interaction and viscosity have opposite effects on ϕ. For $b^2 = \epsilon$, the effect of viscosity is more than the interaction.

In Figs. 9, 10 and 11, the variation of quintessence MGDE potential, Eq. (20), versus redshift is presented for different b^2 and ϵ. Figures 9 and 10 illustrate that: i) for a given b^2 or ϵ, the quintessence MGDE potential $V(\phi)$ decreases during history of the universe. ii) For a given z, $V(\phi)$ increases and decreases with increasing b^2 and ϵ, respectively. Figure 11 shows that in the presence of both interaction and viscosity, although for $b^2 = \epsilon$ at early times the effect of viscosity is more than the interaction, at late times they neutralize the effect of each other.

3 Tachyon MGDE

The energy density and pressure of the tachyon scalar filed are as follows [17]

$$\rho_T = \frac{V(\phi)}{\sqrt{1-\dot{\phi}^2}}, \tag{23}$$

$$p_T = -V(\phi)\sqrt{1-\dot{\phi}^2}. \tag{24}$$

The EoS parameter of the tachyon filed reads

$$\omega_T = \frac{p_T}{\rho_T} = \dot{\phi}^2 - 1. \tag{25}$$

From Eqs. (1) and (23), $\rho_D = \rho_T$ gives the kinetic energy term

$$\dot{\phi}^2 = \frac{\Omega_D - \gamma - \frac{\Omega_k}{3} + \frac{\gamma-1}{\Omega_D}\left(1+\frac{\Omega_k}{3}\right) + 2b^2\left(\frac{1+\Omega_k}{\Omega_D}\right)}{\Omega_D - \gamma - 1} + 3\epsilon. \tag{26}$$

Also using Eqs. (11) and (25), $\omega_D = \omega_T$ yields the tachyon potential

$$V(\phi) = \frac{\alpha^2\Omega_D}{3M_P^2(\Omega_D+\gamma-1)^2}\left[\frac{1 - \frac{\Omega_k}{3} + \frac{\gamma-1}{\Omega_D}\left(1+\frac{\Omega_k}{3}\right) + 2b^2\left(\frac{1+\Omega_k}{\Omega_D}\right)}{1+\gamma-\Omega_D} - 3\epsilon\right]^{1/2}. \tag{27}$$

Integrating Eq. (26) with respect to a and using (36) gives the evolutionary form of the modified ghost tachyon scalar field as

$$\phi(a) - \phi(a_i) = \frac{3M_P^2}{\alpha}\int_{a_i}^{a}(\Omega_D+\gamma-1) \times \left[\frac{\Omega_D - \gamma - \frac{\Omega_k}{3} + \frac{\gamma-1}{\Omega_D}\left(1+\frac{\Omega_k}{3}\right) + 2b^2\left(\frac{1+\Omega_k}{\Omega_D}\right)}{\Omega_D-\gamma-1} + 3\epsilon\right]^{\frac{1}{2}}\frac{\mathrm{d}a}{a}. \tag{28}$$

In Figs. 12, 13 and 14 we plot the variation of ϕ, Eq. (28), versus redshift for different b^2 and ϵ. Also the evolution of tachyon MGDE potential, Eq. (27), is shown in Figs. 15, 16 and 17. Figures 12 to 17 clarify that the scalar field and potential of the tachyon MGDE model behave like the quintessence one (see Figs. 6 to 11).

4 K-essence MGDE

For the K-essence scalar field [18, 19], the pressure

$$p_K(\phi,\chi) = f(\phi)(-\chi+\chi^2), \tag{29}$$

and energy density

$$\rho_K(\phi,\chi) = f(\phi)(-\chi+3\chi^2), \tag{30}$$

give the EoS parameter

$$\omega_K = \frac{p_K}{\rho_K} = \frac{\chi-1}{3\chi-1}, \tag{31}$$

where $\chi = \dot{\phi}^2/2$ is the K-essence kinetic energy. Following Eqs. (11) and (31), $\omega_D = \omega_K$ gives

$$\chi = \frac{2+\gamma-\frac{\Omega_k}{3}+\frac{\gamma-1}{\Omega_D}\left(1+\frac{\Omega_k}{3}\right)+2b^2\left(\frac{1+\Omega_k}{\Omega_D}\right)-\Omega_D+3\epsilon(\Omega_D-\gamma-1)}{4+\gamma-\Omega_k+\frac{\gamma-1}{\Omega_D}(3+\Omega_k)+6b^2\left(\frac{1+\Omega_k}{\Omega_D}\right)-\Omega_D+9\epsilon(\Omega_D-\gamma-1)}. \tag{32}$$

Integrating this with respect to a gives the scalar field of the K-essence MGDE as

$$\phi(a)-\phi(a_i) = \frac{3M_P^2}{\alpha}\int_{a_i}^{a}(\Omega_D+\gamma-1) \times \left[\frac{4+2\gamma-\frac{2\Omega_k}{3}+2\left(\frac{\gamma-1}{\Omega_D}\right)\left(1+\frac{\Omega_k}{3}\right)+4b^2\left(\frac{1+\Omega_k}{\Omega_D}\right)-2\Omega_D+6\epsilon(\Omega_D-\gamma-1)}{4+\gamma-\Omega_k+\left(\frac{\gamma-1}{\Omega_D}\right)(3+\Omega_k)+6b^2\left(\frac{1+\Omega_k}{\Omega_D}\right)-\Omega_D+9\epsilon(\Omega_D-\gamma-1)}\right]^{\frac{1}{2}}\frac{\mathrm{d}a}{a}. \tag{33}$$

The evolutionary behavior of this field for different b^2 and ϵ is plotted in Figs. 18, 19 and 20. Figures present that the K-essence MGDE scalar field increases during history of the universe.

5 Dilaton MGDE

For the dilaton scalar field [20], the pressure and energy density take the forms

$$p_D = -\chi + ce^{\lambda\phi}\chi^2, \tag{34}$$

$$\rho_D = -\chi + 3ce^{\lambda\phi}\chi^2. \tag{35}$$

Here c and λ are two positive constants and $\chi = \dot{\phi}^2/2$ is the dilaton kinetic energy. Therefore, the dilaton EoS parameter reads

$$\omega_D = \frac{p_D}{\rho_D} = \frac{-1+ce^{\lambda\phi}\chi}{-1+3ce^{\lambda\phi}\chi}. \tag{36}$$

Identifying Eq. (11) with (36) reduces to

$$ce^{\lambda\phi}\chi=\frac{2+\gamma-\frac{\Omega_k}{3}+\frac{\gamma-1}{\Omega_D}\left(1+\frac{\Omega_k}{3}\right)+2b^2\left(\frac{1+\Omega_k}{\Omega_D}\right)-\Omega_D+3\epsilon(\Omega_D-\gamma-1)}{4+\gamma-\Omega_k+\frac{\gamma-1}{\Omega_D}(3+\Omega_k)+6b^2\left(\frac{1+\Omega_k}{\Omega_D}\right)-\Omega_D+9\epsilon(\Omega_D-\gamma-1)}. \tag{37}$$

Using $\chi=\dot{\phi}^2/2$ one can take the integral of above equation with respect to a. The result yields

$$\begin{aligned}\phi(a)=\frac{2}{\lambda}\ln\Bigg\{&e^{\frac{\lambda\phi(a_i)}{2}}+\delta\int_{a_i}^{a}(\Omega_D+\gamma-1)\\ \times&\left[\frac{4+2\gamma-\frac{2\Omega_k}{3}+2\left(\frac{\gamma-1}{\Omega_D}\right)\left(1+\frac{\Omega_k}{3}\right)+4b^2\left(\frac{1+\Omega_k}{\Omega_D}\right)-2\Omega_D+6\epsilon(\Omega_D-\gamma-1)}{4+\gamma-\Omega_k+\left(\frac{\gamma-1}{\Omega_D}\right)(3+\Omega_k)+6b^2\left(\frac{1+\Omega_k}{\Omega_D}\right)-\Omega_D+9\epsilon(\Omega_D-\gamma-1)}\right]^{\frac{1}{2}}\frac{\mathrm{d}a}{a}\Bigg\},\end{aligned} \tag{38}$$

where $\delta=\frac{3M_p^2\lambda}{2\alpha\sqrt{c}}$. In Figs. 21, 22 and 23, variation of the dilaton MGDE scalar field, Eq. (38), is illustrated for different b^2 and ϵ. Figures clear that the scalar field of the dilation MGDE model behaves like the K-essence one (see Figs. 18, 19 and 20).

6 Conclusions

Here we studied the Veneziano MGDE model in the framework of Einstein's gravity. We considered a spatially non-flat FRW universe filled with interacting viscous MGDE and DM. We derived a differential equation governing the evolution of the MGDE density parameter and solved it numerically. We also obtained the EoS parameter of the interacting viscous MGDE and the deceleration parameter of the universe. Furthermore, using a correspondence between the interacting viscous MGDE and quintessence, tachyon, K-essence and dilaton scalar field models of DE we reconstructed the dynamics ϕ and potentials $V(\phi)$ of the aforementioned scalar field models according to the evolution of the MGDE density. Our numerical results show the following.

(i) The MGDE density parameter Ω_D for a given coupling constant b^2, increases when the time increases. The evolutionary behavior of Ω_D is independent of viscosity.

(ii) The variation of the deceleration parameter q shows that the universe transitions from an early matter dominant epoch to the de Sitter era in the future, as expected. Also q like Ω_D does not depend on viscosity.

(iii) The EoS parameter ω_D of the MGDE model in the absence of viscosity ($\epsilon=0$), varies from the quintessence phase to the phantom regime. Whereas in the absence of interaction ($b^2=0$), it behaves like the freezing quintessence model. The interaction and viscosity have opposite effects on ω_D.

(iv) The quintessence and tachyon MGDE scalar fields for a given b^2 or ϵ, increase during history of the universe. For a given redshift, they decrease and increase with increasing b^2 and ϵ, respectively. The potentials of the quintessence and tachyon MGDE models for a given b^2 or ϵ, decrease with increasing the time. The interaction and viscosity have opposite effects on both the scalar fields and potentials of the aforementioned models.

(v) The K-essence and dilaton MGDE scalar fields for a given b^2 or ϵ increase during history of the universe.

References

[1] R.G. Cai, Z.L. Tuo, Y.B. Wu, Y.Y. Zhao, Phys. Rev. D **86**, 023511 (2012).

[2] F.R. Urban, A.R. Zhitnitsky, Phys. Rev. D **80**, 063001 (2009);
F.R. Urban, A.R. Zhitnitsky, Phys. Lett. B **688**, 9 (2010);
N. Ohta, Phys. Lett. B **695**, 41 (2011).

[3] E. Witten, Nucl. Phys. B **156**, 269 (1979);
G. Veneziano, Nucl. Phys. B **159**, 213 (1979);
K. Kawarabayashi, N. Ohta, Nucl. Phys. B **175**, 477 (1980);
C. Rosenzweig, J. Schechter, C.G. Trahern, Phys. Rev. D **21**, 3388 (1980);
P. Nath, R.L. Arnowitt, Phys. Rev. D **23**, 473 (1981).

[4] M.M. Forbes, A.R. Zhitnitsky, Phys. Rev. D **78**, 083505 (2008).

[5] R.G. Cai, Z.L. Tuo, H.B. Zhang, arXiv:1011.3212.

[6] E. Ebrahimi, A. Sheykhi, Phys. Lett. B **705**, 19 (2011);
E. Ebrahimi, A. Sheykhi, Int. J. Mod. Phys. D **20**, 2369 (2011);
A. Khodam-Mohammadi, et al., Mod. Phys. Lett. A **27**, 1250100 (2012);
M. Malekjani, A. Khodam-Mohammadi, arXiv:1202.4154;
K. Karami, A. Abdolmaleki, arXiv:1202.2278;
K. Saaidi, arXiv:1202.4097;
K. Saaidi, A. Aghamohammadi, B. Sabet, arXiv:1203.4518.

[7] A. Sheykhi, M. Sadegh Movahed, Gen. Relativ. Gravit. **44**, 449 (2012).

[8] A. Sheykhi, A. Bagheri, Europhys. Lett. **95**, 39001 (2011).

[9] A. Sheykhi, M. Sadegh Movahed, E. Ebrahimi, Astrophys. Space Sci. **339**, 93 (2012).

[10] A. Rozas-Fernandez, Phys. Lett. B **709**, 313 (2012).

[11] W. Zimdahl, D. Pavón, Phys. Lett. B **521**, 133 (2001);
W. Zimdahl, D. Pavón, Gen. Relativ. Gravit. **35**, 413 (2003);
L.P. Chimento, et al., Phys. Rev. D **67**, 083513 (2003).

[12] O. Bertolami, F. Gil Pedro, M. Le Delliou, Phys. Lett. B **654**, 165 (2007).

[13] E.E.O. Ishida, et al., Astropart. Phys. **28**, 547 (2008).

[14] R.R. Caldwell, E.V. Linder, Phys. Rev. Lett. **95**, 141301 (2005).

[15] B. Ratra, J. Peebles, Phys. Rev. D **37**, 321 (1988);
R.R. Caldwell, R. Dave, P.J. Steinhardt, Phys. Rev. Lett. **80**, 1582 (1998).

[16] R.R. Caldwell, Phys. Lett. B **545**, 23 (2002).

[17] A. Sen, JHEP **10**, 008 (1999);
A. Sen, JHEP **04**, 048 (2002);
A. Sen, JHEP **07**, 065 (2002);
E.A. Bergshoeff, et al., JHEP **05**, 009 (2000);
T. Padmanabhan, Phys. Rev. D **66**, 021301 (2002);
T. Padmanabhan, T.R. Choudhury, Phys. Rev. D **66**, 081301 (2002).

[18] T. Chiba, T. Okabe, M. Yamaguchi, Phys. Rev. D **62**, 023511 (2000);
C. Armendáriz-Picón, V. Mukhanov, P.J. Steinhardt, Phys. Rev. Lett. **85**, 4438 (2000);
C. Armendáriz-Picón, V. Mukhanov, P.J. Steinhardt, Phys. Rev. D **63**, 103510 (2001).

[19] C. Armendáriz-Picón, T. Damour, V. Mukhanov, Phys. Lett. B **458**, 209 (1999);
J. Garriga, V. Mukhanov, Phys. Lett. B **458**, 219 (1999).

[20] M. Gasperini, F. Piazza, G. Veneziano, Phys. Rev. D **65**, 023508 (2002);
N. Arkani-Hamed, et al., JCAP **04**, 001 (2004).

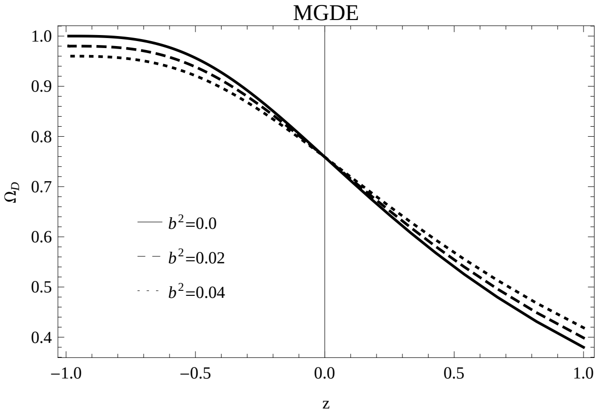

Figure 1: MGDE density parameter, Eq. (14), versus redshift for different coupling constants b^2. Auxiliary parameters are $\Omega_{k_0} = 0.01$, $\Omega_{D_0} = 0.76$ and $\gamma = 1.105$ [1].

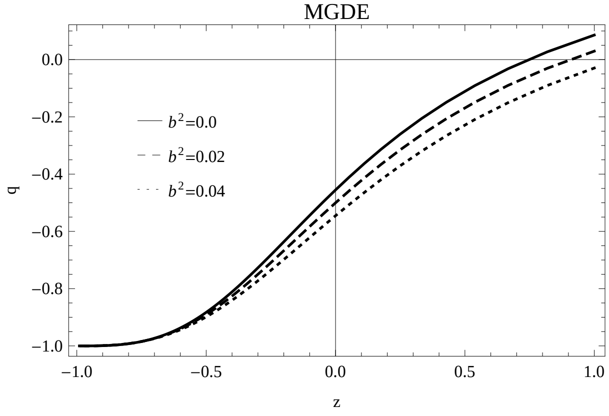

Figure 2: Deceleration parameter, Eq. (13), versus redshift for different coupling constants b^2. Auxiliary parameters as in Fig. 1

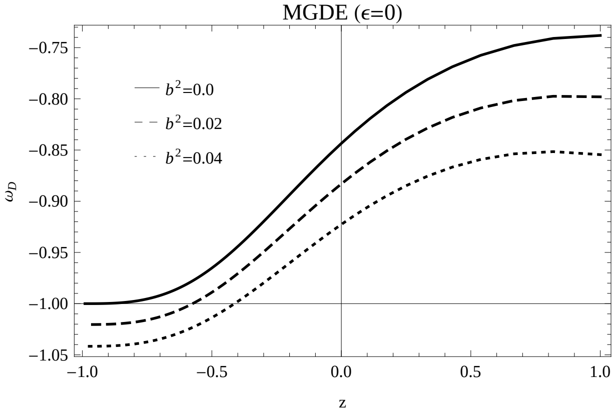

Figure 3: EoS parameter of MGDE, Eq. (11), versus redshift for different coupling constants b^2 with $\epsilon = 0$. Auxiliary parameters as in Fig. 1.

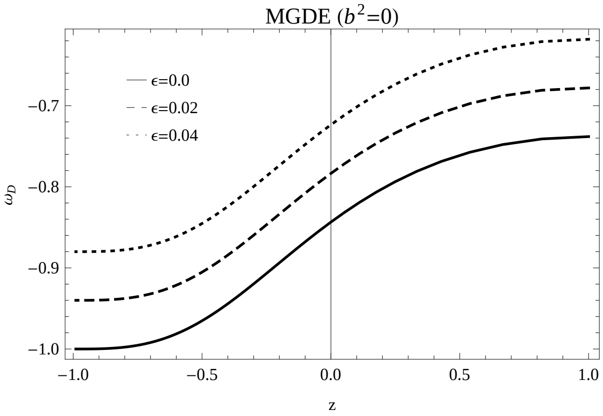

Figure 4: Same as Fig. 3 for different viscosity constants ϵ with $b^2 = 0$.

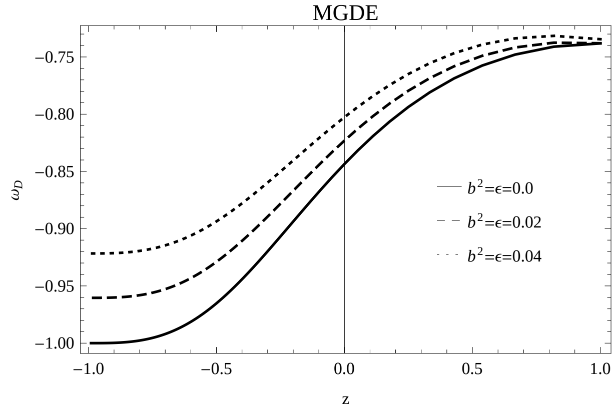

Figure 5: Same as Fig. 3 for different coupling b^2 and viscosity ϵ constants.

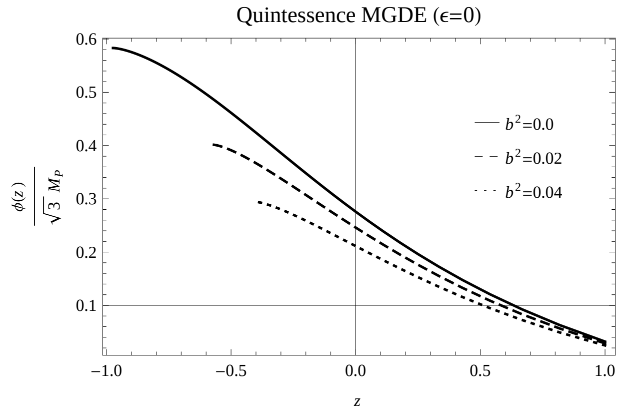

Figure 6: Quintessence MGDE scalar field, Eq. (22), versus redshift for different coupling constants b^2 with $\epsilon = 0$. Auxiliary parameters are $\Omega_{k_0} = 0.01$, $\Omega_{D_0} = 0.76$, $\gamma = 1.105$ [1] and $\phi(1) = 0$.

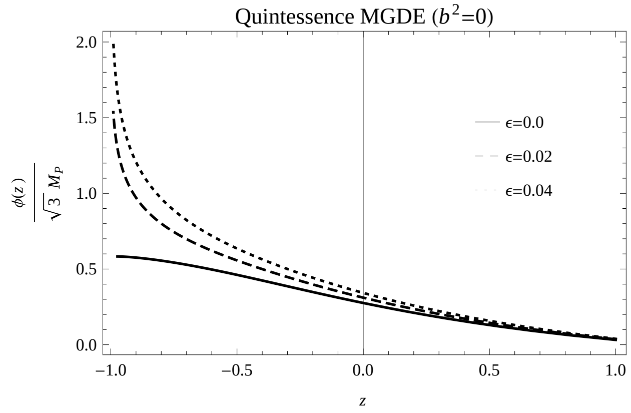

Figure 7: Same as Fig. 6 for different viscosity constants ϵ with $b^2 = 0$.

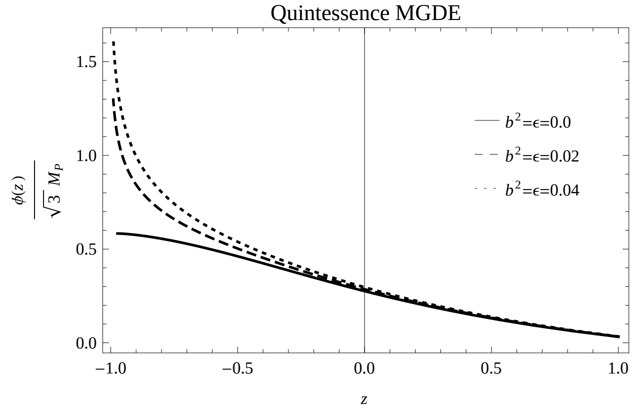

Figure 8: Same as Fig. 6 for different coupling b^2 and viscosity ϵ constants.

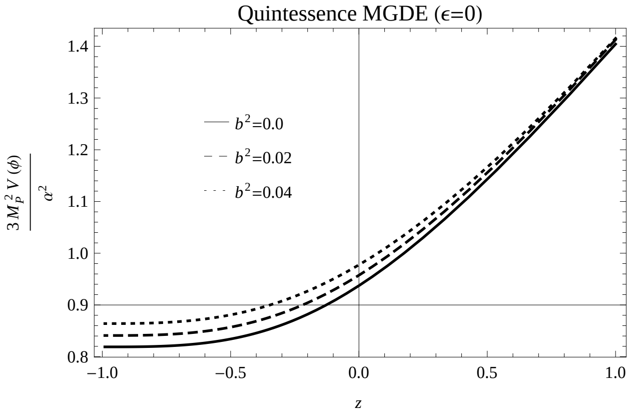

Figure 9: Quintessence MGDE potential, Eq. (20), versus redshift for different coupling constants b^2 with $\epsilon = 0$. Auxiliary parameter as in Fig. 6.

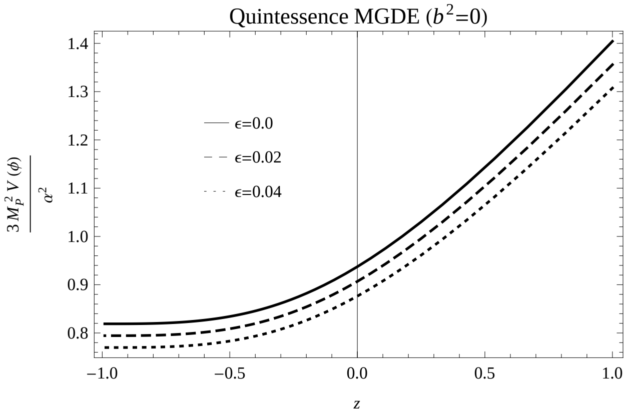

Figure 10: Same as Fig. 9 for different viscosity constants ϵ with $b^2 = 0$. Auxiliary parameters as in Fig. 6.

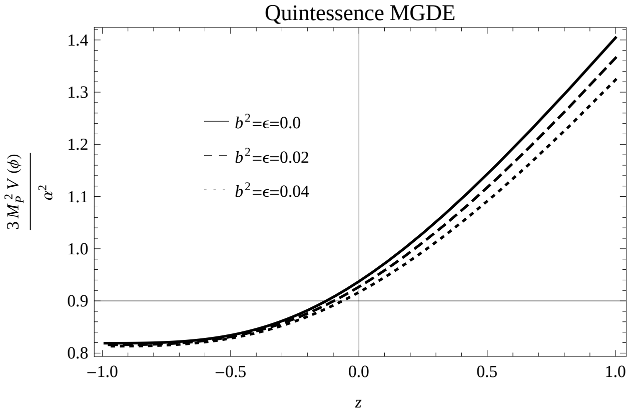

Figure 11: Same as Fig. 9 for different coupling b^2 and viscosity ϵ constants. Auxiliary parameters as in Fig. 6.

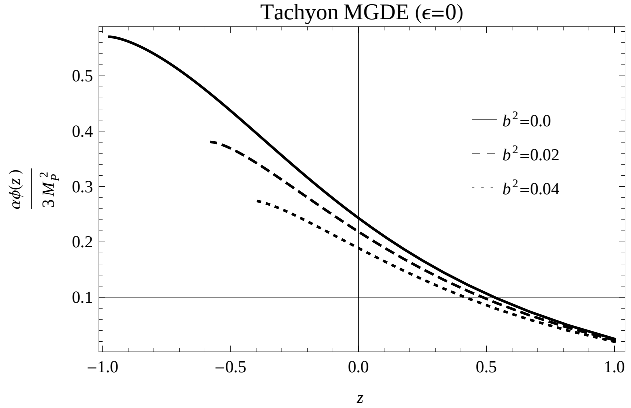

Figure 12: Tachyon MGDE scalar field, Eq. (28), versus redshift for different coupling constants b^2 with $\epsilon = 0$. Auxiliary parameters as in Fig. 6.

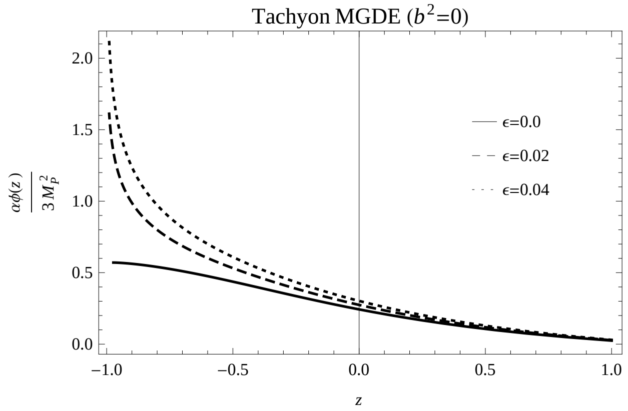

Figure 13: Same as Fig. 12 for different viscosity constants ϵ with $b^2 = 0$.

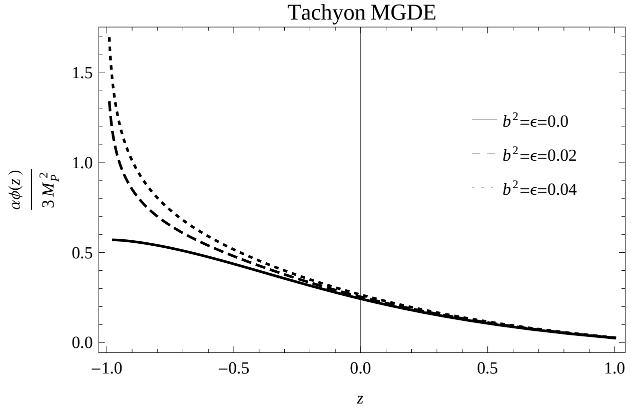

Figure 14: Same as Fig. 12 for different coupling b^2 and viscosity ϵ constants.

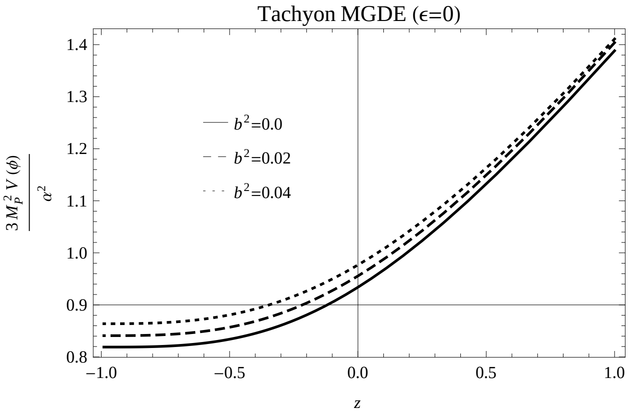

Figure 15: Tachyon MGDE potential, Eq. (27), versus redshift for different coupling constants b^2 with $\epsilon = 0$. Auxiliary parameter as in Fig. 6.

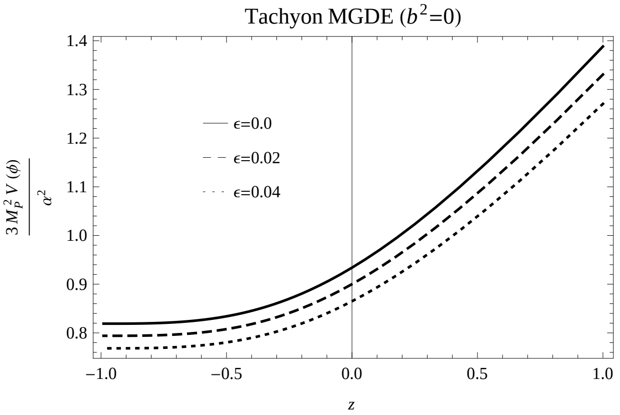

Figure 16: Same as Fig. 15 for different viscosity constants ϵ with $b^2 = 0$.

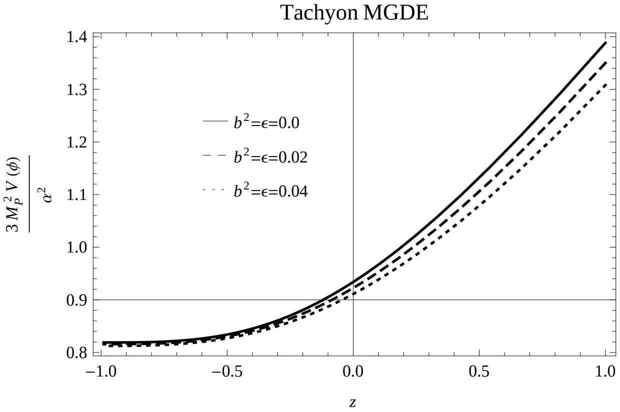

Figure 17: Same as Fig. 15 for different coupling b^2 and viscosity ϵ constants.

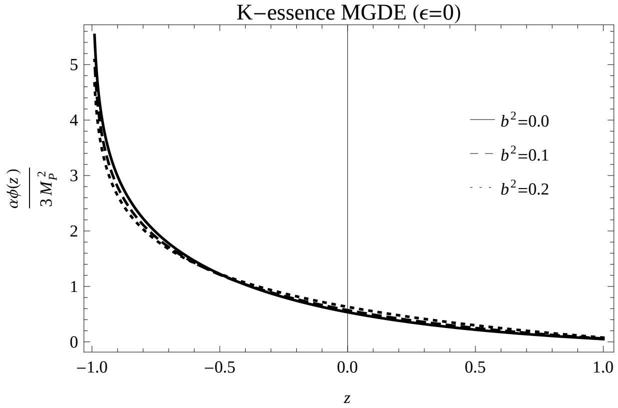

Figure 18: K-essence MGDE scalar field, Eq. (33), versus redshift for different coupling constants b^2 with $\epsilon = 0$. Auxiliary parameters as in Fig. 6.

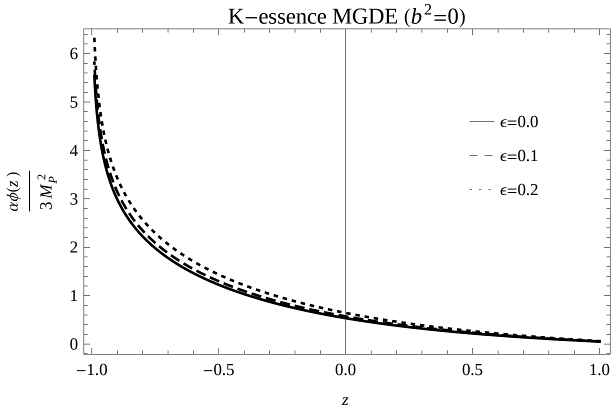

Figure 19: Same as Fig. 18 for different viscosity constants ϵ with $b^2 = 0$.

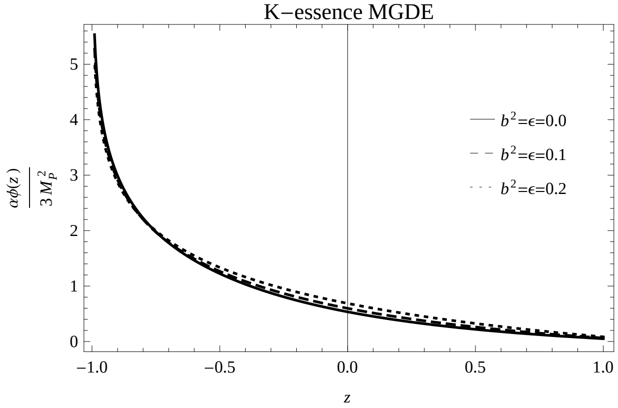

Figure 20: Same as Fig. 18 for different coupling b^2 and viscosity ϵ constants.

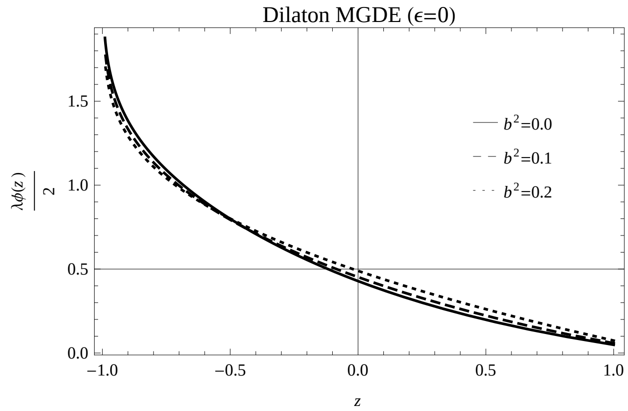

Figure 21: Dilaton MGDE scalar field, Eq. (38), versus redshift for different coupling constants b^2 with $\epsilon = 0$. Auxiliary parameters are $\Omega_{k_0} = 0.01$, $\Omega_{D_0} = 0.76$, $\gamma = 1.105$ [1], $\phi(1) = 0$ and $\delta = \frac{3M_p^2\lambda}{2\alpha\sqrt{c}} = 1$.

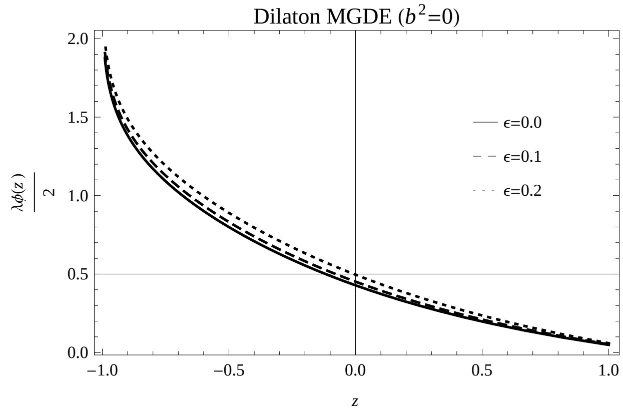

Figure 22: Same as Fig. 21 for different viscosity constants ϵ with $b^2 = 0$.

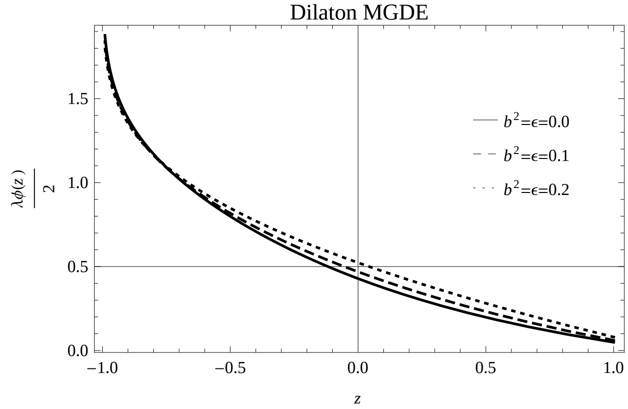

Figure 23: Same as Fig. 21 for different coupling b^2 and viscosity ϵ constants.